Analysis and Design of Boolean Associative Memories Made of Resonant Oscillator Arrays

Paolo Maffezzoni, *Senior Member, IEEE*, Bichoy Bahr, *Student Member, IEEE*, Zheng Zhang, *Member, IEEE*, and Luca Daniel, *Member, IEEE*

***Abstract*—This paper investigates some relevant open issues related to implementing Boolean associative memories using oscillator arrays. At the circuit level, the employment of a class of MEMS-based oscillators which is ideal for large arrays realizations is herein considered. At the system level, the crucial problems of array connectivity and spurious patterns generation are explored in detail. As a result, an enhanced training rule is proposed which is able to simplify the array architecture while improving memory association capability.**

***Index Terms*—Cognitive memory, MEMS oscillators, pattern recognition, phase-domain modeling.**

I. Introduction

ARRAYS OF coupled oscillators are now attracting huge interest for the realization of brain-inspired computing machines implementing associative memories [1]–[4]. The main advantage of these machines is their unprecedented potentiality compared to sequential digital computers in processing problems which are massively parallel in nature, such as data classification and recognition.

Emerging nano-fabrication technologies, such as MEMS [6], [7], metal-oxide [8]–[10], spin-torque devices [11], [12], and memristors [13]–[15], are expected to allow manufacturing large oscillator arrays in a few years. Nevertheless, realizing oscillator-array associative memories by hardware still remains extremely challenging. At the circuit level, open issues include finding suitable oscillator devices and proper coupling methods. At the system level, open issues include how to encode the information within the array (e.g., using oscillators frequency or phase) as well as finding suitable array architectures and training algorithms. In the last years, compact oscillator models and efficient computational tools for the analysis of oscillator arrays have been developed [16]–[20]. They are expected to play a key role in solving the open problems at both levels.

In this paper, we focus on the family of boolean associative memories having *regeneration capability*, i.e., being able to regenerate the correct output pattern even though the input stimulus pattern is distorted or incomplete. Such memories have many applications in pattern recognition and cryptography. Boolean associative memories can be implemented with oscillator arrays where the encoded information is decided by the oscillators relative phase differences achieved at synchronization [1], [2], [12].

The feasibility of arrays made of CMOS resonant LC oscillators have been recently investigated [19]. However, the large area occupied by the inductance poses severe restrictions on the number of oscillators that can be integrated in standard CMOS technology. Another critical issue is how to determine the proper number of connections among oscillators. Some architectures with a few connections limited to nearest neighbors oscillators tend to give small information storage capability [21]. By contrast, a highly-interconnected architecture can give larger storage capability at the price of higher area occupation and power dissipation. More importantly, a highly-interconnected array is prone to produce spurious output patterns during the recognition/regeneration step. These faults are caused by some unwanted equilibrium points that are not associated to any memorized pattern. This work extends previous research [2], [12], [19] by addressing some of the above-mentioned unsolved issues. Specifically, the novel contributions of this paper include:

1) We consider the employment of an emerging class of MEMS-based oscillators, referred to as resonant body oscillators (RBOs) ideal for large oscillator arrays realizations. For this class of devices, we present an efficient phase-domain modeling and simulation framework that allows asserting the associative memory capability of the array. We describe how such capability indeed depends on the proper selection of RBO circuit nodes employed to implement mutual couplings.
2) We investigate in details the mechanism of spurious patterns generation by finding how it is associated to the presence of critical "chain-like" connections among some of the oscillators in the array.
3) Thanks to this understanding, we are able to provide an enhanced training rule that can significantly reduce the spurious patterns while removing many unnecessary couplings. The novel algorithm leads to pattern-dependent partially-interconnected array architectures with a few nonlocal connections. In addition, it provides a practical criterion to determine the maximum number of patterns that can be memorized in the array for a given number of oscillators.

Manuscript received April 22, 2016; revised June 30, 2016; accepted July 26, 2016. This paper was recommended by Associate Editor T. Serrano-Gotarredona.

P. Maffezzoni is with Politecnico di Milano, DEIB, I20133 Milan, Italy (e-mail: pmaffezz@elet.polimi.it).

B. Bahr, Z. Zhang, and L. Daniel are with Massachusetts Institute of Technology (MIT), Cambridge, MA 02139 USA (e-mail: bichoy@mit.edu; z_zhang@mit.edu; luca@mit.edu).

Color versions of one or more of the figures in this paper are available online at http://ieeexplore.ieee.org.

Digital Object Identifier 10.1109/TCSI.2016.2596300

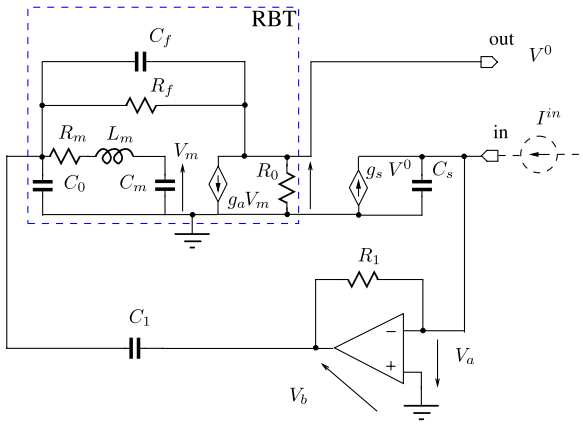

Fig. 1. RBO circuit model: it includes a resonant body transistor (RBT) [6] followed by a phase shifter and a loop amplifier. Label "out" denotes the output node employed to read the oscillator response while "in" denotes the input node used for current injection.

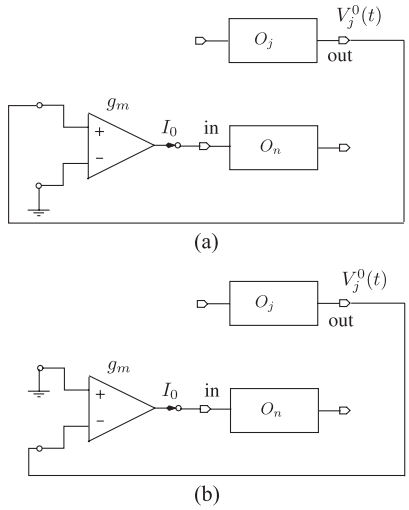

Fig. 2. Detail of the coupling circuit between the nth and jth oscillators: (a) positive coupling $g_{nj} = g_m$; (b) negative coupling $g_{nj} = -g_m$.

These contributions are organized as follows: Section II describes the RBO model, the coupling circuit and proves memory association ability. In Section III, we investigate the phenomenon of spurious path mechanism, while in Section IV we provide the enhanced training algorithm. Finally, Section V is devoted to numerical experiments.

II. RBO Associative Memory

RBOs are ultra-compact and low-power harmonic oscillators that are monolithically integrated inside CMOS process. At the heart of the RBO is the CMOS-MEMS resonant body transistor (RBT). These are truly solid-state MEMS resonators, completely encapsulated inside the solid CMOS die. RBTs are fabricated with regular MOS transistors and circuits as part of the standard CMOS process, without any post-processing, or special packaging requirements [5]. RBTs are capable of achieving moderate quality factors $(Q \sim 30)$ at high-frequencies ($>$ 10 GHz), with a foot-print smaller than 10 μm^2 [6]. This enables the realization of RBOs at 10 GHz, with power consumption on the order of 2 mW in a 100 μm^2 area. The ultra-compact form-factor enables the realization of large RBO clusters suitable for large oscillator arrays implementation. In particular, the monolithic integration *inside* the CMOS die leverages the multiple back-end-of-line metal layers available, allowing sophisticated routing and inter-connection as required for complex oscillator coupling that are otherwise unfeasible. Furthermore, the high-frequency operation ensures high throughput from the oscillator cluster memory, which together with the low power consumptions, results in highly power efficient system with small energy per inference performance. Fig. 1 shows the circuit model of the RBO that we will use in our analysis where the RBT is described by the small-signal model reported in the box in Fig. 1. The RBT model consists of a mechanical resonator described by a RLC branch, followed by a MOS transistor of transconductance g_α. Elements C_f and R_f represent feedthrough parasitics [6]. The RBT is connected to a block (described, at behavioral level, with a transconductance g_s and a capacitor C_s) implementing a $\pi/2$ phase shifter, followed by an amplification stage in an oscillator feedback loop. When properly dimensioned, the RBO exhibits harmonic oscillatory responses at angular frequency ω_0.

In order to construct an oscillator array, N such RBOs are weakly coupled through transconductance elements g_{nj} implemented with transconductance amplifiers [22], as shown in Fig. 2. The amplifier reads the output voltage $V_j^0(t)$ of the jth oscillator and injects a proportional current $I_0 = g_{nj} V_j^0(t)$ into the nth oscillator. In practical implementations, buffers (not shown in Fig. 2) can be inserted at the output and input terminals of the oscillators to isolate them from transconductance amplifier loading effects. The strength of coupling is determined by amplifier transconductance factor g_m while its sign is decided by the amplifier terminal used for reading the oscillator output voltage, as shown in Fig. 2.

The associative memory capability of RBO arrays critically depends on the way the output and injecting nodes are selected. The analysis developed in this section and the simulations illustrated in Section V show that a proper selection consists in using the drain of the RBT in Fig. 1 as the oscillator output node and the input terminal of the loop amplifier as the current injecting node. The small-amplitude harmonic output voltage $V^0(t) = V_M \cos(\omega_0 t)$ is ideal to drive the transconductance amplifier and realize weak coupling while the selected injection point yields great phase sensitivity thus favoring mutual synchronization. The resulting array architecture is shown in Fig. 3 and will be referred to as a *fully-interconnected* array if $g_{nj} \neq 0$ for any j and n with $j \neq n$, or as a *partially-interconnected* array if $g_{nj} = 0$ for some $n \neq j$.

Under weak coupling condition, the response of the whole array can be described with a phase-domain model where the output voltage of the nth oscillator

$$V_n^0(t) = V_M \cos\left(\omega_0 t + \phi_n(t)\right) \tag{1}$$

is determined by its time-varying excess phase $\phi_n(t)$ [16]–[18].

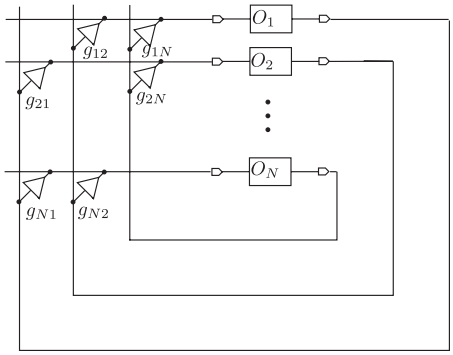

Fig. 3. Oscillator array with transconductance couplings.

The array response is governed by the following nonlinear equations:

$$\dot{\phi}_n(t) = \omega_0 \Gamma_M \cos\left(\omega_0 t + \phi_n(t) + \delta\right) I_n^{\text{in}}(t) \tag{2a}$$

$$I_n^{\text{in}}(t) = \sum_{j=1}^{N} g_{nj} V_M \cos\left(\omega_0 t + \phi_j(t)\right) \tag{2b}$$

where the periodically-varying function

$$\Gamma(t) = \Gamma_M \cos(\omega_0 t + \delta) \tag{3}$$

has been used to describe the oscillator phase sensitivity to the injected current $I_n^{\text{in}}(t)$ [23]–[26]. For RBOs such a phase sensitivity is a sinusoid with a relative phase difference δ with respect to the output voltage $V^0(t)$. In what follows we show how to realize oscillator arrays having associative memory capability such a relative phase difference should be $\delta = \pi/2$, i.e., the output voltage and sensitivity function waveforms should be in quadrature. To assert this capability, we substitute (2b) into (2a) and use averaging [27], obtaining

$$\dot{\phi}_n(t) = \omega_0 \frac{\Gamma_M V_M}{2} \sum_{j=1}^{N} g_{nj} \cos\left(\phi_n(t) - \phi_j(t) + \delta\right). \tag{4}$$

By denoting $\delta = \pi/2 - \epsilon$ (where ϵ measures the distance from being in quadrature), (4) can be recast into

$$\dot{\phi}_n(t) = H_0 \sum_{j=1}^{N} s_{nj} \sin\left(\phi_j(t) - \phi_n(t) + \epsilon\right) \tag{5}$$

which is quite similar to the well-known *Kuramoto*'s model [28], where

$$s_{nj} = \omega_0 \frac{\Gamma_M V_M}{2H_0} g_{nj} \tag{6}$$

are the coupling coefficients and H_0 is a scaling factor. By introducing the functions

$$H_{nj}(\chi) = H_0 s_{nj} \sin(\chi + \epsilon) \tag{7}$$

it is easy to verify that if coupling coefficients are selected symmetric, i.e., $s_{nj} = s_{jn}$, (i.e., if coupling between any couple of oscillators is bilateral and symmetric $g_{nj} = g_{jn}$) and provided that $\epsilon = 0$,[1] then the function $H_{nj}(\chi)$ satisfies the property $H_{nj}(-\chi) = -H_{jn}(\chi)$ and thus the convergence theorem for oscillatory neural networks applies [1, p. 285]. This theorem states that the phase model (5) is the gradient of the energy function

$$U(\phi_1, \phi_2, \ldots, \phi_N) = -H_0 \sum_n \sum_j s_{nj} \cos(\phi_j - \phi_n). \tag{8}$$

As a consequence, provided that oscillators remain synchronized in frequency, the array dynamics is such that the phase variables $(\phi_1(t), \phi_2(t), \phi_N(t))$, always converge to an equilibrium point, with $\dot{\phi}_1(t) = \cdots = \dot{\phi}_N(t) = 0$, which is a local minimum of $U(\phi_1, \phi_2, \ldots, \phi_N)$.

Such constant relative phase differences achieved at steady-state can be used to store information. In a boolean memory, a couple of (almost) in-phase oscillators, i.e., having phase difference $\phi_n(t) - \phi_j(t) \approx 0$, are conventionally assumed to store a $+1$ while a couple of (almost) anti-phase oscillators, i.e., with phase difference $\phi_n(t) - \phi_j(t) \approx \pi$, are conventionally assumed to store a -1.

An array of N oscillators can store a binary word (describing a pattern) $\vec{w} = \{b_1, \ldots, b_N\}$ where the value of the nth bit $b_n \in (-1, 1)$ is decided by

$$b_n = \text{sign}\left\{\cos\left[\phi_n(t) - \phi_1(t)\right]\right\} \tag{9}$$

with $b_1 = +1$.

A single word $\vec{w}$ can be encoded into the array by setting coupling coefficients according to the rule [1]

$$s_{nj} = b_n b_j. \tag{10}$$

Coefficients setting (10) corresponds to an energy function U with a single minimum for phase difference values $\Delta\phi_{nj} = \phi_n(t) - \phi_j(t)$ that are either 0 or π. Setting (10) can thus be employed to initialize the array to any new input word $\vec{w} = \{b_1, \ldots, b_N\}$ that should be recognized.

Similarly, a set of p words

$$\vec{w}^k = \left\{b_1^k, b_2^k, \ldots, b_N^k\right\} \tag{11}$$

with $k = 1, \ldots, p$ can be memorized into the array by setting the coupling coefficients with the well known *Hebbian rule* [1]

$$s_{nj} = \frac{1}{p} \sum_{k=1}^{p} b_n^k b_j^k. \tag{12}$$

Setting (12) corresponds to an energy function U having a local minimum for each memorized word.

As a conclusion, the association/recognition of an input word is accomplished through a two step procedure. In the first step, referred to as *Initialization*, the bits of the word to be recognized are loaded into the coupling coefficients according to setting (10). In this condition, oscillators array is allowed to synchronize. In the second step, referred to as *Recognition*, the coupling coefficients are switched to setting (12), accounting

[1]It is worth noting that for $\epsilon \neq 0$, it results $\sin(-\chi + \epsilon) \neq -\sin(\chi + \epsilon)$ and thus the hypothesis of the convergence theorem does not hold anymore. In practice the violation of the quadrature condition corresponds to a progressive deterioration or completely lost of the associative memory capability.

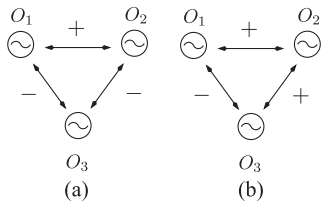

Fig. 4. Elementary chains composed of three oscillators: (a) with an even number of negative connections; (b) with an odd number of negative connections.

for all memorized words. In this condition, and provided that oscillators keep synchronized, the relative phase differences achieved during Initialization evolve towards the local minimum of U which is closest according to the internal "metric." The final phase differences reached at steady state along with (9) determine the recognized output word.

III. Spurious Patterns and Critical Chains

Oscillator arrays trained with Hebbian rule present some critical features. A first criticality is due to the fact that both coupling settings (10) and (12) for initialization and recognition steps, respectively, lead to a fully-interconnected network. As a consequence, a large number $N \times (N-1)$ of transconductance amplifiers are needed to implement coupling with a large area and high power dissipation. A second and more tricky criticality is due to the fact that fully-interconnected arrays with variable coupling values, i.e., $s_{nj} \neq 0$ for any n and $j \neq n$, tend to give energy functions U with undesired spurious local minima not corresponding to any memorized pattern. This can produce memory association faults.

To better investigate this second issue, we present the following discussion summarized in four points:

1) A robust encoding with rule (9) of a set of boolean words should be such that the local minima of the energy function U occur for phase difference values close to zero or to π, i.e., $\Delta\phi_{nj} \approx 0$ or $\Delta\phi_{nj} \approx \pi$. Vice versa, spurious pattern associations can occur when the local minima of U are placed at phase difference values distributed over the interval $(0, \pi)$. In this case, some input errors in the bits of the word to be recognized or the unavoidable errors due to numerical finite precision of simulation can drive the array dynamics into one of such unwanted minima.
2) We focus on elementary chain arrays composed of three coupled oscillators like the ones shown in Fig. 4. We first observe that a positive coupling coefficient s_{nj} between two oscillators correspond to an excitatory coupling that tends to keep the two oscillators in phase, similarly a negative s_{nj} corresponds to an inhibitory coupling that tends to keep the two oscillators in anti-phase. In fact, such relative phase differences minimize the energy function U by contributing negative terms $-H_0 s_{nj} \cos(\phi_j - \phi_n)$ to (8).

   With this premise, we can show that when the number of negative connections in the chain is even (i.e., 0 or 2) then the local minima of U occur only for $\Delta\phi_{nj} \approx 0$ or $\Delta\phi_{nj} \approx \pi$. By contrast, when the number of negative connections in the chain is odd (i.e., 1 or 3), then the local minima of U correspond to phase differences critically distributed over $(0, \pi)$. Fig. 4(a) shows an elementary chain with an even number of negative connections while Fig. 5 reports the associated energy function U, calculated with (8), as a function of the relative phase differences $\phi_2 - \phi_1$ and $\phi_3 - \phi_1$. The minima of these function occur for $\phi_2 - \phi_1 = 0$ (i.e., O_1 and O_2 are in phase) and for $\phi_3 - \phi_1 = \pm\pi$ (i.e., O_3 is in anti-phase with O_1 and thus with O_2). In other words, in-phase and anti-phase relationships satisfy the excitatory/inhibitory coupling constraints in an elementary chain with an even number of negative connections. This conclusion does not hold for an elementary chain with an odd number of negative connections, as that one shown in Fig. 4(b). In fact, let us start from O_1 and move clockwise along the chain: according to the sign of connections, O_2 would oscillate in phase with O_1, O_3 would be in phase with O_2 and thus O_3 would be in phase with O_1. However, this last condition collides with the direct negative connection existing between O_3 and O_1. Fig. 6 shows the energy function U for the array in Fig. 4(b) and confirms that, in this case, equilibrium phase differences are critically distributed, i.e., $\phi_3 - \phi_1 = \pi/3$ and $\phi_2 - \phi_1 = -\pi/3$. We observe how the analysis above continues to hold if the three oscillators

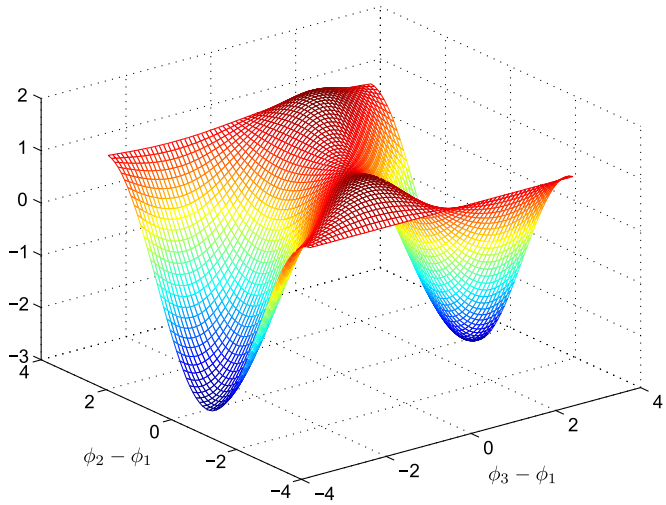

Fig. 5. Energy function U for the chain array in Fig. 4(a).

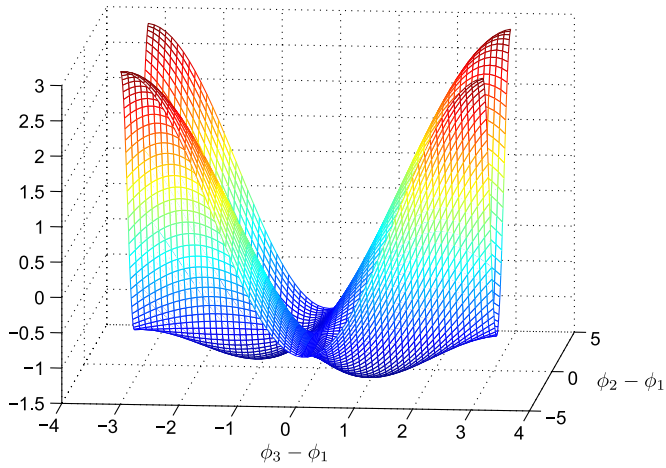

Fig. 6. Energy function U for the chain array in Fig. 4(b).

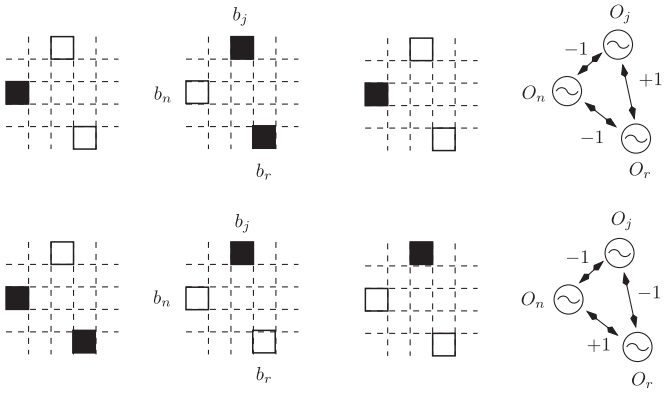

Fig. 7. Two sequence of patterns where bits b_n, b_j, and b_r are strongly correlated.

forming the chain are selected within a large array made of N oscillators. In fact, even though oscillators from O_4 to O_N will add new terms to the energy function (8), these extra terms do not contain the phase differences $\phi_2(t) - \phi_1(t)$ and $\phi_3(t) - \phi_1(t)$. As a result, the energy function dependence on $\phi_2(t) - \phi_1(t)$ and $\phi_3(t) - \phi_1(t)$ will remain that shown in Figs. 5 and 6. We conclude that whenever three oscillators within an array form a critical elementary chain with an odd numbers of negative connections, spurious patterns can potentially occur.

3) According to Hebbian rule (12), the coupling coefficient between two oscillators, with index n and j, measures the correlation between the bits b_n and b_j over the p memorized patterns. If such bits are strongly correlated in-phase, i.e., $b_n^k b_j^k = 1$ or in anti-phase, i.e., $b_n^k b_j^k = -1$, for all of the p patterns, then coupling coefficient s_{nj} will saturate to $+1$ or -1, respectively. Vice versa, when such bits are weakly correlated over a given set of patterns, i.e., for some k $b_n^k b_j^k = 1$ and for some other $b_n^k b_j^k = -1$, then the coupling coefficient s_{nj} will assume a fractional value.
4) It is possible to show how elementary chains storing strongly correlated bits of a word (over a given set of patterns) can only contain an even number of negative connections. This property can be proved by observing that the three bits, let's say b_n, b_j, and b_r, have only two possible ways to be correlated. In the first way, the three bits are equal $b_n = b_j = b_r$ and thus the three interconnection couplings are all positives. In the second way, two of the three bits are equal and opposite to the remaining one. This second way, which includes the three cases $b_n = -b_j = b_r$, $-b_n = b_j = b_r$, and $b_n = b_j = -b_r$, leads to two negative connection coefficients and one positive. Fig. 7 shows two examples where each couple of bits (over the three training patterns) are strongly correlated according to the second possible way explained above. In this figure, white boxes indicate $+1$ bits while black boxes indicate -1 bits, the values of the resulting coupling coefficients are reported on the right. For instance, in the first example reported on top of Fig. 7, bit b_j has always the same sign as b_r and the opposite sign of b_n. This results in coupling coefficients that saturate to +1 or to -1 with the number of such negative connections being even.

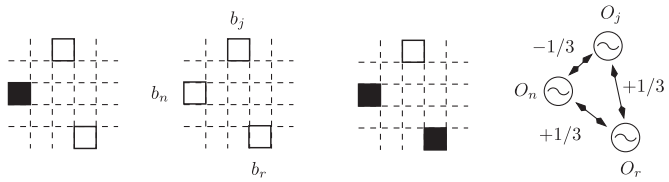

Fig. 8. A sequence of three patterns where bits b_n, b_j, and b_r are weakly correlated.

By contrast, elementary chains storing weakly correlated bits (over a given set of patterns) can contain an odd number of negative connections. This is the case for the example shown in Fig. 8 where bits b_n and b_j have opposite sign in the first and third patterns while they have the same sign in the second pattern. This leads to fractional coupling coefficients and to a critical chain array with a odd number of negative connections.

The conclusion of the analysis presented above is that: *critical chains responsible for spurious patterns can be removed by keeping only couplings coefficients $+1$ and -1 between oscillators storing strongly correlated bits.*

IV. Enhanced Training Method

Thanks to the understanding gained in the previous section, we are now in the position to present an enhanced training procedure. It consists in iteratively considering patterns subsets

$$\begin{aligned} \text{Set}_{1,} &= \{\vec{w}^1\} \\ \text{Set}_2 &= \{\vec{w}^1, \vec{w}^2\} \\ &\cdots \\ \text{Set}_k &= \{\vec{w}^1, \vec{w}^2, \vec{w}^k\} \end{aligned} \tag{13}$$

of increasing dimension $k \leq p$.

For each subset Set_k, coupling coefficients s_{nj} are first com puted with the standard Hebbian rule (12) extended to the k patterns, and then are updated according to the following pruning rule:

$$s_{nj}^{(k)} = \begin{cases} +1 & \text{if} \quad s_{nj} = +1 \\ -1 & \text{if} \quad s_{nj} = -1 \\ 0 & \text{if} \quad -1 < s_{nj} < +1 \end{cases} \tag{14}$$

that leads to *pattern-dependent partially-interconnected* arrays. In the array obtained at kth iteration, connections are not necessarily among nearest neighbor oscillators. Furthermore, the number of coupling connections can vary significantly from one oscillator to another.

We denote $\nu_{\text{ave}}(k)$ the average number of coupling connections that one oscillator has in the array (averaging is done over all oscillators that form the array), and $\nu_{\min}(k)$ the minimum number of connections of the "less connected" oscillator in the array. At the first iteration $k = 1$, i.e., when a single pattern is memorized in the array, all connections are either $s_{nj}^{(1)} = s_{nj} = +1$ or $s_{nj}^{(1)} = s_{nj} = -1$ and $\nu_{\text{ave}}(1) = \nu_{\min}(1) = N - 1$. When k is increased, the rule (14) tends to remove some connections and thus both $\nu_{\text{ave}}(k)$ and $\nu_{\min}(k)$ decrease with $\nu_{\min}(k) < \nu_{\text{ave}}(k) < N - 1$. The procedure is stopped when condition $\nu_{\min}(k) = 0$ occurs. This condition occurs when one or more oscillators in the array are isolated

(they have no connections at all) meaning that the associated bits of the input word cannot be regenerated by the associative memory. The proposed iterative procedure yields a partially-interconnected array, with an average $N \times \nu_{\text{ave}}(k)$ number of couplings of values $+1$ and -1 (i.e., that can be implemented with transconductance amplifiers having all the same gain g_m), and a practical criterion to fix the maximum number of patterns that can be stored and retrieved in/from the memory.

So far we have focused on the memory capability to regenerate a corrupted input word. In some cases, recognition requires to know the index of the memorized pattern that gives the best degree of match (BDOM) with the input word. Commonly this operation needs further elaboration and extra hardware [12].

With the proposed training procedure, instead, we are able to show how the BDOM can be efficiently deduced by directly looking at the relative phase differences achieved during the recognition step, thus eliminating the need for extra circuits. To explain the method, we observe that the addition of any new word $\vec{w}^{k+1}$ during the step from the kth to the $(k+1)$th iteration, should necessarily corresponds to the elimination of at least one coupling s_{nj}. This means that there exists a couple of indices n_k and j_k for which

$$\begin{aligned} s^{(k)}_{n_k,j_k} &= \pm 1 \\ s^{(k+1)}_{n_k,j_k} &= 0 \end{aligned} \tag{15}$$

due to the fact that the associated bits b_{n_k} and b_{j_k} are strongly correlated over the first k words but they are not on the first $k+1$ ones, i.e.,

$$a_k = \text{sign}\left[b^{(k+1)}_{n_k}\, b^{(k+1)}_{j_k}\right] \neq \text{sign}\left[s^{(k)}_{n_k,j_k}\right]. \tag{16}$$

At each iteration of the training procedure, the information about n_k, j_k, and the sign a_k are computed and stored. This information along with the phase differences values reached during the Recognition step of a new input word, define the BDOM

$$\text{BDOM}_k = \text{sign}\left[\cos(\phi_{n_k} - \phi_{j_k})\right] \cdot a_k \tag{17}$$

with respect to the words forming the set Set_{k+1}.

If $\text{BDOM}_k = +1$ it means that limitedly to Set_{k+1}, the pattern $\vec{w}^{k+1}$ is the one that best matches the input word to be recognized. Vice versa, if $\text{BDOM}_k = -1$ it means that the best matching word belongs to the set of smaller size $\text{Set}_{k+1} \setminus \{\vec{w}^{k+1}\} = \text{Set}_k$. As a consequence, the highest index k_m for which $\text{BDOM}_{k_m} = +1$ corresponds to the best matching word $\vec{w}^{k_m+1}$. This last observation concludes the description of the proposed training procedure for the Recognition step.

It remains to see how array connectivity can be simplified during the Initialization step. To address this last issue, we propose the following pruning rule to simplify coupling coefficients s_{nj} computed with (10)

$$s^0_{nj} = \begin{cases} s_{nj} & \text{if} \quad j = 1 \\ 0 & \text{if} \quad j \neq 1 \end{cases} \tag{18}$$

The rule above, adopted for the Initialization step, leads to a *star network* having as center the reference oscillator O_1. The reference oscillator is connected unilaterally to the other $N-1$ oscillators through coupling coefficients $s^0_{n1} = b_n b_1 = \pm 1$ that impose the relative phase differences of the word to be recognized.

TABLE I
RBO PARAMETERS

Parameter	Value
C_0	14 fF
R_m	88 kΩ
L_m	28 μH
C_m	9 aF
C_f	0.22 fF
R_f	1 MΩ
R_0	20 kΩ
C_s	16 fF
R_1	100 kΩ
C_1	100 fF
g_α	-1μS
g_s	1mS

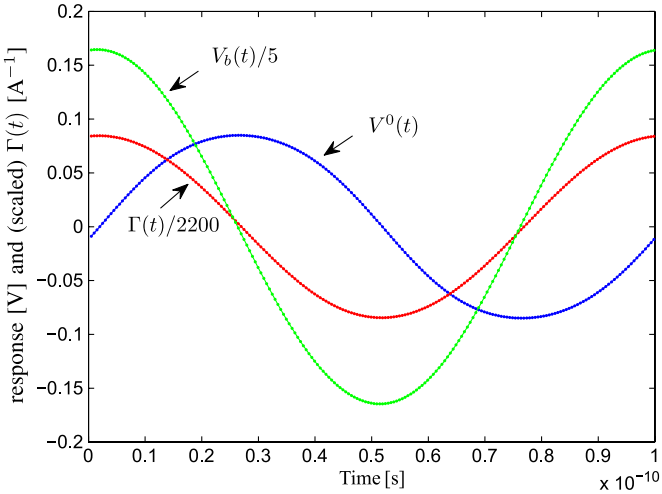

Fig. 9. RBO free-running response $V^0(t)$, voltage $V_b(t)$ at the output of the loop amplifier, and sensitivity function $\Gamma(t)$ to current injection at the input node.

V. Numerical Examples

The steady-state response of a single RBO, with the circuit model shown in Fig. 1 and the parameters reported in Table I, is first simulated. The loop operation amplifier is described as a nonlinear block with the input-output relationship

$$V_b = V_{\text{lim}} \tanh\left(\frac{A_v}{V_{\text{lim}}} V_a\right) \tag{19}$$

where $A_v = 10$ is the amplification and $V_{\text{lim}} = 2.0$ V is the voltage supply.

The RBO circuit oscillates at frequency $\omega_0/(2\pi) = 10$ GHz. Fig. 9 shows the output voltage $V^0(t)$ at the RBT drain and the phase-sensitivity curve for an injected current entering into the input node: *the two curves are sinusoids with the prescribed $\pi/2$ relative phase shift requested to form oscillator arrays with associative memory capability*. Fig. 9 also reports the (scaled) voltage $V_b(t)$ at the output of the RBO loop amplifier. We observe how $V_b(t)$ is in phase and not in quadrature with the sensitivity $\Gamma(t)$ (for the selected injecting node) and thus it is completely unsuitable to form oscillator arrays having associative memory capability.

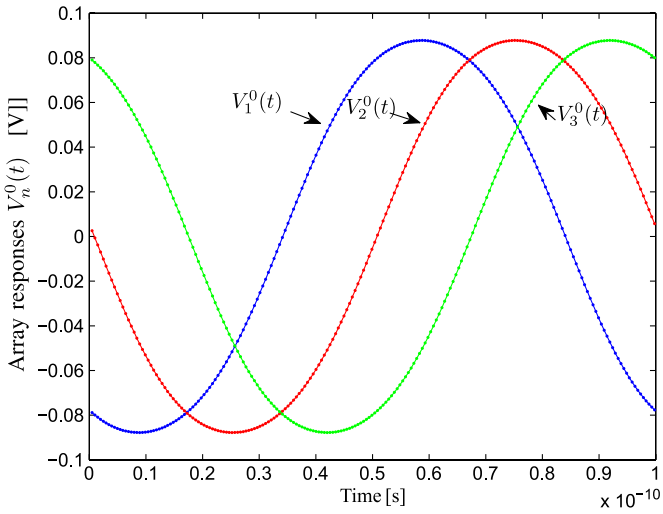

Fig. 10. Steady-state response of the elementary chain array in Fig. 4(b).

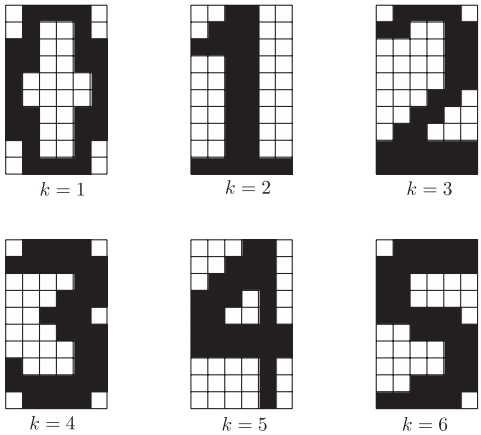

Fig. 11. Patterns to be memorized.

As a preliminary example, we analyze the output response of the elementary chain array shown in Fig. 4(b). Oscillators are weakly coupled through bilateral transconductances of magnitude $g_{nj} = 20\ \mu$S and with the signs described in Fig. 4(b), i.e., a single negative connection is realized between O_1 and O_3 while other connections are positive. From the array response obtained with detailed circuit-level simulations as shown in Fig. 10 and from a comparison with Fig. 9, we are led to the following conclusions: i) for weakly coupled oscillator arrays, amplitude modulation effects are indeed negligible, ii) the relative phase differences among oscillators are $\pi/3$ and its multiples as predicted by the phase-domain analysis, thus confirming that this chain array is critical for boolean associative memories.

Hence, we proceed to analyze an oscillator array made of 60 coupled RBOs where, as illustrative example, we want to memorize a set of boolean words described by the patterns reported in Fig. 11 [29]. The 10×6 binary image pixels are associated to the 60 oscillators in a column-wise way starting from the top-left hand pixel which corresponds to O_1. Two cases are considered: a) a fully-interconnected architecture where coupling coefficients are determined with the standard Hebbian rule (12), b) a partially-interconnected architecture where coupling coefficients are found with the proposed

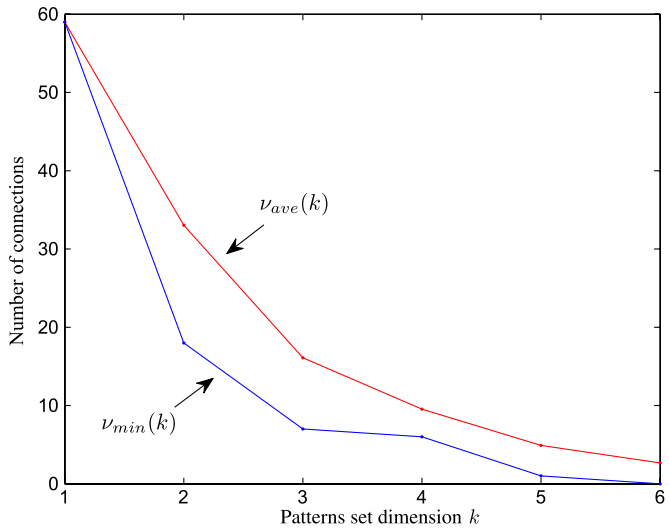

Fig. 12. Average and minimum number of oscillator connections as a function of the patterns set dimension.

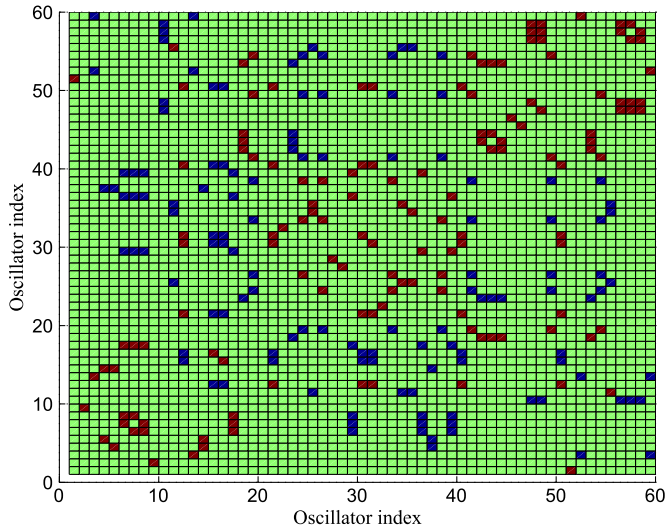

Fig. 13. Connection matrix of the partially-connected array.

iterative procedure based on rule (14). In Case a), the array has $N \times (N-1) = 3540$ coupling connections. In Case b) instead Fig. 12 reports the average and minimum number of connections ν_{ave} and ν_{min} that one oscillator has in the array as a function of the patterns set dimension k.

For $k = 5$, i.e., for a set including the first five images shown in Fig. 11, we find $\nu_{\text{min}} = 1$ and $\nu_{\text{ave}} \approx 4.4$. This means that for the given number of oscillators $N = 60$ and given patterns, $k = 5$ is the maximum number of words that can be completely regenerated by the associative memory.[2] In fact, for $k = 6$ it results $\nu_{\text{min}} = 0$ with three oscillators that are isolated Fig. 13 shows a picture of the $N \times N$ connection matrix, for $k = 5$ stored patterns, where the presence of a (nonzero) coupling $s_{nj} = \pm 1$ is indicated with a dark box at position (n, j). Connection matrix is quite sparse with only 260 coupling connections.

[2]The maximum number of patterns that can be stored and correctly retrieved by the memory indeed depends on the type of patterns to be memorized.

TABLE II
SUCCESS RATE IN RECOGNITION

k	Partially-int.	Fully-int.
2	100%	100%
3	100%	97%
4	100%	16%
5	98%	0%

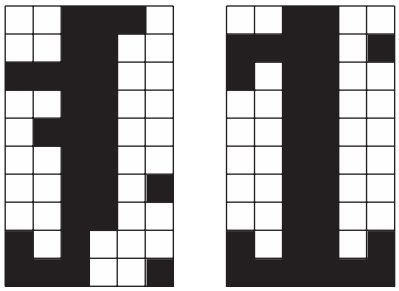

Fig. 14. (Left-hand side) corrupted Input "1"; (right-hand side) wrong Output word supplied by the fully-interconnected array trained over $k = 4$ patterns: only a subset of the corrupted bits are correctly regenerated.

Hebbian rule adopted to train oscillator arrays is just an heuristic and it does not always guarantee successful storage of patterns. For this reason, extensive simulations of the fully and partially interconnected arrays are needed to check and compare associative memory performance. To this aim, we repeat a sufficiently large number of simulations (i.e., 200 runs) where the Input patterns are generated from the memorized ones by corrupting (i.e., a $+1$ bit is transformed into a -1 and vice versa) ten randomly selected bits (i.e., the pattern and the bits are selected randomly with uniform probability). From the simulated responses, we calculate the success rate in recognition as a function of the number k of memorized patterns. A pattern is successfully recognized by the arrays when all of the bits are correctly regenerated. In our simulations, we also consider 10% random variations of the coupling transconductance values g_{nj} that account for potential mismatch of the circuit components.

Table II shows the simulation results: for $k = 2$ and $k = 3$, the partially interconnected and the fully-interconnected arrays are both very close to 100% successful recognition. For $k = 4$, instead the fully-interconnected array has a dramatic deterioration of its associative memory capability. Fig. 14-(right-hand side) shows, as an example, the Output word generated by the fully-interconnected array when the corrupted Input pattern "1" shown in Fig. 14-(left-hand side) is applied: the array correctly regenerates only some of the corrupted bits. By contrast, Fig. 15 shows the successful Output produced by the partially-interconnected array for the same Input.

For $k = 5$, the fully-interconnected array has no more recognition capability and it always converges to spurious Output patterns. As an example, Fig. 16-(right-hand side) shows the Output word generated by the fully-interconnected array for $k = 5$ when the corrupted Input pattern "2" in Fig. 16-(left-hand side) is applied. For such a case, Fig. 17 also shows how the phase variables $\phi_n(t)$ of the fully-interconnected array evolve during the Recognition step: starting from the 0 or $\pm\pi$ values achieved during the Initialization step, phase variables tend to be critically distributed over the whole $(-\pi, \pi)$ interval.

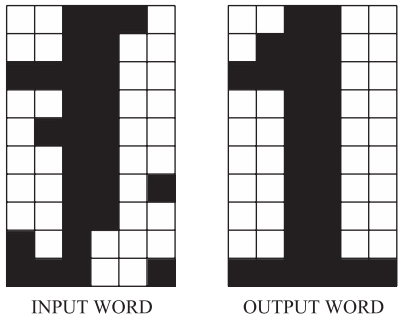

Fig. 15. (Left-hand side) corrupted Input "a"; (right-hand side) correct Output word supplied by the partially-interconnected array trained over $k = 4$ patterns.

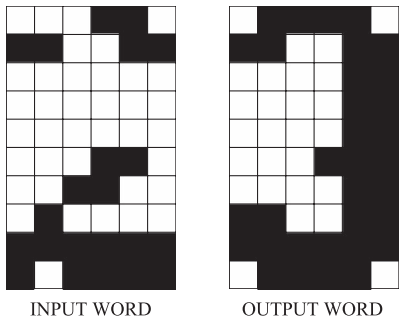

Fig. 16. (Left-hand side) corrupted Input "2"; (right-hand side) wrong Output word supplied by the fully-interconnected array for $k = 5$: this spurious word is a mix of images "0," "2," and "3."

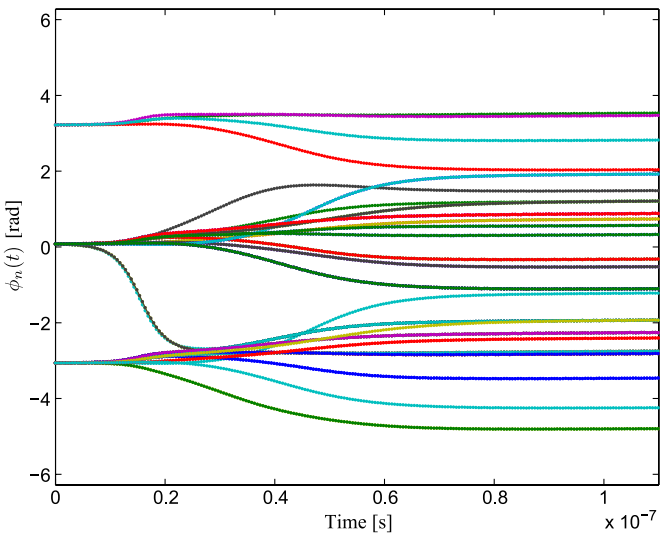

Fig. 17. Phase variables during the Recognition step in the fully-interconnected array for $k = 5$.

By contrast, when the corrupted Input word is applied to the partially-interconnected array, the phase variables during the Recognition step shown in Fig. 18 approach steady-state values that are close to either 0 or π (or $-\pi$).

When the steady-state phase differences in Fig. 18 are plugged in (9), they lead to the correct output word shown in Fig. 19-(right-hand side). Fig. 19 also reports the BDOM vector: correctly, the highest index with a $+1$ is for $k_m = 2$ meaning that $k_m + 1 = 3$ is the index of the pattern in Fig. 11 that best matches the input word.

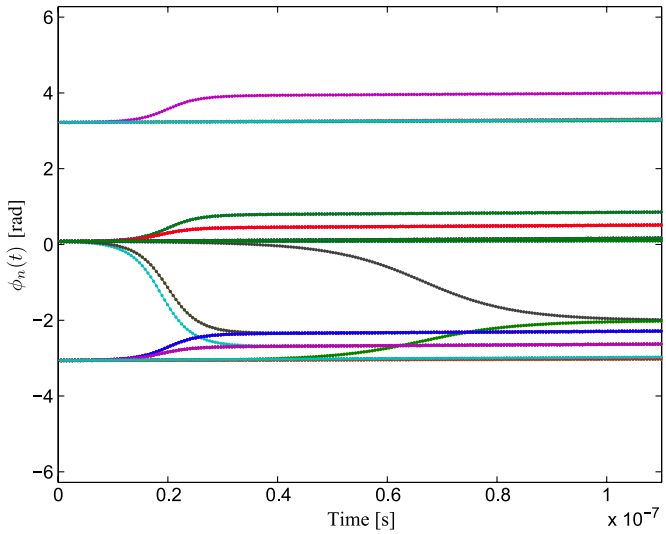

Fig. 18. Phase variables during the Recognition step in the partially-interconnected array for $k = 5$.

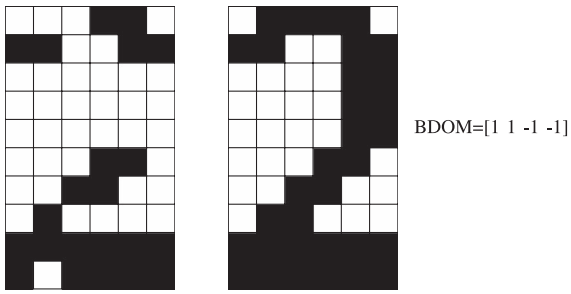

Fig. 19. (Left-hand side) corrupted Input "2"; (right-hand side) correct Output word supplied by the partially-interconnected array for $k = 5$.

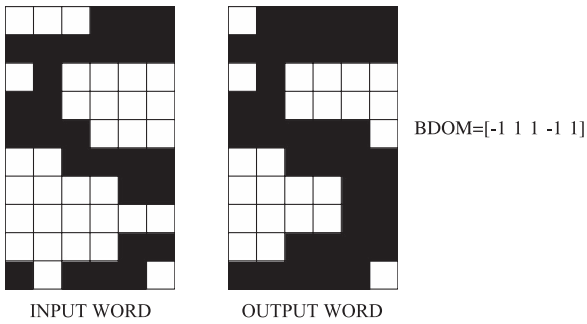

Fig. 20. (Left-hand side) corrupted Input "5"; (right-hand side) Output word supplied by the partially-interconnected array for $k = 6$.

As a final example, we show what happens when all six patterns in Fig. 11 are memorized in the array with the proposed training method. In this case, three oscillators remain isolated and the whole array has only 190 coupling connections. The application of the corrupted Input pattern "5" shown in Fig. 20-(left-hand side) results into the output word shown in Fig. 20-(right-hand side): the array is able to correctly regenerate the word with the exception of the third pixel which corresponds to one of the isolated oscillators. The BDOM vector has a $+1$ at $k_m = 5$ which correctly identifies the best matching word in the pattern with index $k_m + 1 = 6$. Therefore, even though the regeneration capability is lost in some bits, the array continues to correctly recognize the input word.

VI. Conclusion

In this paper, we have analyzed some relevant design issues regarding the realization of boolean associative memories using large oscillator arrays. An efficient phase-domain modeling approach has been exploited to investigate the behavior of arrays made of MEMS-based oscillators. We have proved that the associative memory capability of such systems indeed depends on the oscillator nodes that are employed to implement mutual coupling. Besides that, we have investigated the tricky mechanism of spurious patterns generation that in many cases can deteriorate the memory performance and cause association faults. We have shown how spurious patterns are due to the presence of critical interconnections among oscillators storing weakly correlated bits. An improved training method has been presented which consists in removing many of such critical interconnections. This yields a simplification of the array architecture and reduces the occurrence of spurious patterns. We have shown how the array of resonant oscillators, when trained with the proposed algorithm, is able to regenerate corrected patterns from corrupted input words. Furthermore, we have described how the proposed algorithm can provide the index of the memorized pattern that best matches the input word to be recognized.

References

[1] F. C. Hoppensteadt and E. M. Izhikevich, *Weakly Connected Neural Networks*. New York, NY, USA: Springer-Verlag, 1997.

[2] F. Corinto, M. Bonnin, and M. Gilli, "Weakly connected oscillatory network models for associative and dynamic memories," *Int. J. Bifurcation Chaos*, vol. 17, no. 12, pp. 4365–4379, Dec. 2007.

[3] M. Mirchev, L. Basnarkov, F. Corinto, and L. Kocarev, "Cooperative phenomena in networks of oscillators with non-identical interactions and dynamics," *IEEE Trans. Circuits Syst. I, Reg. Papers*, vol. 61, no. 3, pp. 811–819, Mar. 2014.

[4] K. Kostorz, R. W. Holzel, and K. Krischer, "Distributed coupling complexity in a weakly coupled oscillatory network with associative properties," *New J. Phys.*, vol. 15, no. 8, pp. 0830100(1)–0830100(14), Aug. 2013.

[5] B. Bahr, R. Marathe, and D. Weinstein, "Theory and design of phononic crystals for unreleased CMOS-MEMS resonant body transistors," *J. Microelectromech. Syst.*, vol. 24, no. 5, pp. 1520–1532, Oct. 2015.

[6] R. Marathe, B. Bahr, W. Wang, Z. Mahmood, L. Daniel, and D. Weinstein, "Resonant body transistors in IBMs 32 nm SOI CMOS technology," *J. Microelectromech. Syst.*, vol. 23, no. 3, pp. 636–650, Jun. 2014.

[7] J. Juillard, P. Prache, and N. Barniol, "Analysis of mutually injection-locked oscillators for differential resonant sensing," *IEEE Trans. Circuits Syst. I, Reg. Papers*, vol. 63, no. 7, pp. 1055–1066, Jul. 2016.

[8] S. Datta, N. Shukla, M. Cotter, A. Parihar, and A. Raychowdhury, "Neuro inspired computing with coupled relaxation oscillators," in *Proc. DAC*, Jun. 2014, pp. 1–6.

[9] N. Shukla *et al.*, "Synchronized charge oscillations in correlated electron systems," *Nat. Sci. Rep.*, vol. 4, pp. 1–6, 2014.

[10] P. Maffezzoni, L. Daniel, N. Shukla, S. Datta, and A. Raychowdhury, "Modeling and simulation of vanadium dioxide relaxation oscillators," *IEEE Trans. Circuits Syst. I, Reg. Papers*, vol. 62, no. 9, pp. 2207–2215, Sep. 2015.

[11] S. P. Levitan, Y. Fang, D. H. Dash, T. Shibata, D. E. Nikonov, and G. I. Bourianoff, "Non-Boolean associative architectures based on nano-oscillators," in *Proc. 13th Int. Workshop CNNA*, 2012, pp. 1–6.

[12] D. E. Nikonov, G. Csaba, W. Porod, T. Shibata, D. Voils, D. Hammerstrom, I. A. Young, and G. I. Bourianoff, "Coupled-oscillator associative memory array operation for pattern recognition," *IEEE J. Exploratory Solid-State Comput. Devices Circuits*, vol. 1, no. 1, pp. 85–93, Dec. 2015.

[13] H. Wang *et al.*, "PPV modeling of memristor-based oscillators and application to ONN pattern recognition," *IEEE Trans. Circuits Syst. II, Express Briefs*, 2016. [Online]. Available: http://ieeexplore.ieee.org/

[14] A. Buscarino *et al.*, "Turing patterns in memristive cellular nonlinear networks," *IEEE Trans. Circuits Syst. I, Reg. Papers*, 2016. [Online]. Available: http://ieeexplore.ieee.org/

[15] A. Ascoli, S. Slesazeck, H. Mahne, R. Tetzlaff, and T. Mikolajick, "Nonlinear dynamics of a locally-active memristor," *IEEE Trans. Circuits Syst. I, Reg. Papers*, vol. 64, no. 2, pp. 1165–1174, Feb. 2015.
[16] D. Harutyunyan, J. Rommes, J. ter Maten, and W. Schilders, "Simulation of mutually coupled oscillators using nonlinear phase macromodels applications," *IEEE Trans. Comput.-Aided-Des. Integr. Circuits Syst.*, vol. 28, no. 10, pp. 1456–1466, Oct. 2009.
[17] M. Bonnin and F. Corinto, "Phase noise and noise induced frequency shift in stochastic nonlinear oscillators" *IEEE Trans. Circuits Syst. I, Reg. Papers*, vol. 60, no. 8, pp. 2104–2115, Aug. 2013.
[18] P. Maffezzoni, B. Bahr, Z. Zhang, and L. Daniel, "Analysis and design of weakly coupled oscillator arrays based on phase-domain macromodels," *IEEE Trans. Comput.-Aided-Des. Integr. Circuits Syst.*, vol. 34, no. 1, pp. 77–85, Jan. 2015.
[19] P. Maffezzoni, B. Bahr, Z. Zhang, and L. Daniel, "Oscillator array models for associative memory and pattern recognition," *IEEE Trans. Circuits Syst. I, Reg. Papers*, vol. 62, no. 6, pp. 1591–1598, Jun. 2015.
[20] P. Maffezzoni, B. Bahr, Z. Zhang, and L. Daniel, "Reducing phase noise in multi-phase oscillators," *IEEE Trans. Circuits Syst. I, Reg. Papers*, vol. 63, no. 3, pp. 379–388, Mar. 2016.
[21] T. C. Jackson, A. A. Sharma, J. A. Bain, J. A. Weldon, and L. Pileggi, "Oscillatory neural networks based on TMO nano-oscillators and multi-level RRAM cells," *IEEE J. Emerg. Sel. Topics Circuits Syst.*, vol. 5, no. 2, pp. 230–241, Jun. 2015.
[22] M. Gustavsson, J. J. Wikner, and N. Nianxiong Tan, *CMOS Data Converter for Communications*, vol. 543. New York, NY, USA: Springer International Series in Engineering and Computer Science, 2000.
[23] F. X. Kaertner, "Analysis of white and $f^{-\alpha}$ noise in oscillators," *Int. J. Circuit Theory Appl.*, vol. 18, pp. 485–519, 1990.
[24] A. Demir, A. Mehrotra, and J. Roychowdhury, "Phase noise in oscillators: A unifying theory and numerical methods for characterisation," *IEEE Trans. Circuits Syst. I, Fundam. Theory Appl.*, vol. 47, no. 5, pp. 655–674, May 2000.
[25] P. Maffezzoni, "Analysis of oscillator injection locking through phase-domain impulse-response," *IEEE Trans. Circuits Syst. I, Reg. Papers*, vol. 55, no. 5, pp. 1297–1305, Jun. 2008.
[26] S. Levantino and P. Maffezzoni, "Computing the perturbation-projection-vector of oscillators via frequency domain analysis," *IEEE Trans. Comput.-Aided-Des. Integr. Circuits Syst.*, vol. 31, no. 10, pp. 1499–1507, Oct. 2012.
[27] P. Vanassche, G. Gielen, and W. Sansen, "On the difference between two widely publicized methods for analyzing oscillator phase behavior," in *Proc. ICCAD*, Nov. 2002, pp. 229–233.
[28] J. A. Acebrn, L. L. Bonilla, C. J. P. Vicente, F. Ritort, and R. Spigler, "The Kuramoto model: A simple paradigm for synchronization phenomena," *Rev. Mod. Phys.*, vol. 77, pp. 137–185, Jan. 2005.
[29] F. C. Hoppensteadt and E. M. Izhikevich, "Oscillatory neurocomputers with dynamic connectivity," *Phys. Rev. Lett.*, vol. 82, pp. 2983–2986, 1999.

Paolo Maffezzoni (M'08–SM'15) received the Laurea degree (summa cum laude) in electrical engineering from Politecnico di Milano, Italy, in 1991 and the Ph.D. degree in electronic instrumentation from Universita' di Brescia, Italy, in 1996. Since 1998, he has been with Politecnico di Milano, where he is an Associate Professor of Electrical Engineering. His current research interests include modeling and simulation of oscillatory devices for engineering applications, synchronization phenomena, nonlinear circuits and systems, analog and mixed-signal electronics, stochastic simulation, unconventional computing. He has over 125 research publications among which 65 papers in international journals. He currently serves as an Associate Editor for the IEEE TRANSACTIONS ON CIRCUITS AND SYSTEMS—PART I: REGULAR PAPERS. He has served as an Associate Editor for IEEE TRANSACTIONS ON COMPUTER-AIDED DESIGN OF INTEGRATED CIRCUITS AND SYSTEMS and as a member of the Technical Program Committee for the IEEE/ACM Design Automation Conference.

Bichoy Bahr (S'10) received his M.Sc. and B.Sc. degrees both in electrical engineering from Ain Shams University, Cairo, Egypt, in 2008 and 2012, respectively, and the Ph.D degree in electrical engineering and computer science from Massachusetts Institute of Technology (MIT), Cambridge, MA, USA, in 2016. He is currently with Kilby Labs, Texas Instruments, Dallas, TX, USA. Dr. Bahr was with the Hybrid MEMS group at MIT from 2012 to 2016 and with MEMS-Vision LLC, Egypt, from 2009 to 2012. He received the 2016 Doctoral Dissertation Seminar Award (best dissertation award) from the Microsystems Technology Laboratory (MTL) of MIT. His research interests include the design, fabrication, modeling and numerical optimization of monolithically integrated unreleased MEMS resonators, in standard ICs technology. He is also interested in multi-GHz MEMS-based monolithic oscillators, frequency synthesizers, coupled oscillator-arrays, and unconventional signal processing.

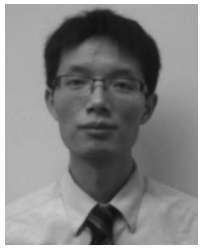

Zheng Zhang (S'09–M'15) received the B.Eng. degree in electronics from Huazhong University of Science and Technology, Wuhan, China in 2008, the M.Phil. degree in electrical and electronic engineering from the University of Hong Kong, Hong Kong, in 2010, and the Ph.D. degree in electrical engineering and computer science from Massachusetts Institute of Technology (MIT), Cambridge, MA, USA, in 2015. He is currently a Postdoc Associate with the Research Laboratory of Electronics at MIT. His research interests include high-dimensional uncertainty quantification, tensors, and data analysis. Applications of interest include nano-scale devices, circuits and systems, energy systems, and biomedical computation. Dr. Zhang received the 2016 ACM SIGDA Outstanding Ph.D. Dissertation Award in Electronic Design Automation, the 2015 Doctoral Dissertation Seminar Award from the Microsystems Technology Laboratory of MIT, the 2014 Best Paper Award from IEEE TRANSACTIONS ON COMPUTER-AIDED DESIGN OF INTEGRATED CIRCUITS AND SYSTEMS, the 2011 Li Ka Shing Prize (university best M.Phil/Ph.D thesis award) from the University of Hong Kong, the 2016 SPI best conference paper award, and three additional best paper nominations in international conferences. His industrial research experiences include Coventor Inc. and Maxim-IC.

Luca Daniel (S'98–M'03) received the Ph.D. degree in electrical engineering from the University of California, Berkeley, CA, USA, in 2003. He is currently a Full Professor in the Electrical Engineering and Computer Science Department of the Massachusetts Institute of Technology, Cambridge, MA, USA (MIT). Industry experiences include HP Research Labs, Palo Alto, CA, USA (1998) and Cadence Berkeley Labs, CA, USA (2001). His current research interests include integral equation solvers, uncertainty quantification and parameterized model order reduction, applied to RF circuits, silicon photonics, MEMs, magnetic resonance imaging scanners, and the human cardiovascular system. Prof. Daniel was the recipient of the 1999 IEEE TRANSACTIONS ON POWER ELECTRONICS best paper award; the 2003 best Ph.D. thesis awards from the Electrical Engineering and the Applied Math departments at UC Berkeley; the 2003 ACM Outstanding Ph.D. Dissertation Award in Electronic Design Automation; the 2009 IBM Corporation Faculty Award; the 2010 IEEE Early Career Award in Electronic Design Automation; the 2014 IEEE TRANSACTIONS ON COMPUTER-AIDED DESIGN OF INTEGRATED CIRCUITS AND SYSTEMS best paper award; and ten awards in conferences.

Prof. Daniel recently received the 2016 Teaching Award from the MIT School of Engineering.